KOPIO

Technical Note #059

Neutron rates in the downstream beampipe charged particle veto & the detector

Laurence Littenberg

Physics Department
Brookhaven National Laboratory
Upton, N.Y. 11973 USA

8 July 2003

1. Introduction

It is necessary to develop better criteria for properties of the charged particle vetoes in the downstream beampipe. We know something about the neutron halo rates from Jaap Doornbos' recent technical notes[1−3]. This note explores how these can be used to estimate the rates in the charged particle veto counters so that one can figure out how far from the beam one can stand to place these counters.

We are mainly concerned with the total rate, since this is what determines the random veto loss. We assume that considerations of veto blindness can be addressed through adequate segmentation of the veto counters, and need not be discussed here.

Note that one fact that hasn't been much discussed is that one must compare neutron-induced rates with the rate of charged particles from kaon decays in the beam. It's pointless to try to reduce the former to far below the latter. For a rough estimate of the latter, note that we are assuming ~14 million decays/sec in the fiducial decay region. The DS beam pipe section is about half as long as the decay region so that there are roughly 7M decays in it. Since about 80% of these decays contain charged particles, one would expect ~ 5.6 Megahertz in these counters. David Jaffe improved on this by invoking the fast Monte Carlo to calculate the number of events/microbunch that put at least one charged track into the DS beampipe CPV. He found a rate corresponding to 6.12 MHz (see Fig. 1.1).

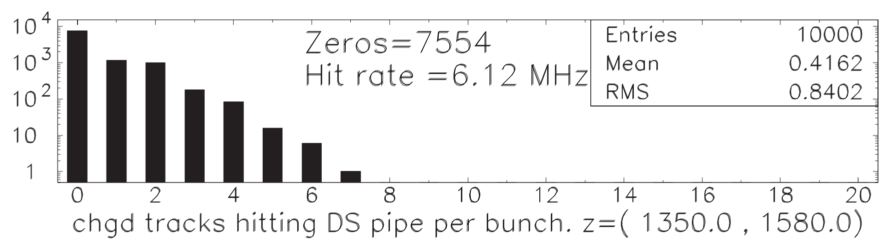

Figure 1.1: Fast MC calculation of charged particle hit distribution in the DS beampipe CPV due to K_L decays

Note that this corresponds to 70TP on target and a 2.4 second spill. I'd like to design for 100TP, in which case the optimum is a 2.7 second spill. In this case we need to multiply David's rate by $\frac{100}{70} \times \frac{2.4}{2.7} = 1.27$. This yields 7.77 MHz. This gives a scale. One has to keep in mind, however, that a fair fraction of this rate has already been taken into account in the optimization of the spill length. That is, we are already ditching a lot of the μbunches in which these charged particles occur. The neutron random veto effect will be additional.

Most readers will want to skip the next few pages (with the possible exception of Table 3.1), which are mainly included for checking purposes and to start from Section 3.3.

2. Sensitivity to angle

Imagine a single counter of length L, width w and thickness t situated above the beam. If all neutrons came directly along the z-axis, the rate in the counter would be

$$R = \int f(x, y) \left(1 - e^{-\frac{L}{\lambda}}\right) dxdy \tag{2.1}$$

where λ is the interaction length in the scintillator and the transverse spatial distribution of halo neutrons is given by $f(x, y)$. For a counter 200 cm long, and $\lambda \approx 100$ cm, this would come to $0.865fwt$ in the approximation that f is constant in the region of the counter. If we take $t = 0.3$cm, this yields $R = 0.26fw$.

However the neutrons don't really strike the counter end-on. The next level of approximation is to assume that all neutrons strike it at the same angle, α, and that this angle is completely in the y-z plane. The path length through the counter material will then be $t/sin\alpha$. The probability of interaction will consequently be $1 - e^{-\frac{t}{\lambda sin\alpha}}$. Neutrons from a vertical interval $L\tan\alpha$ will impinge in the counter (see Fig. 2.1).

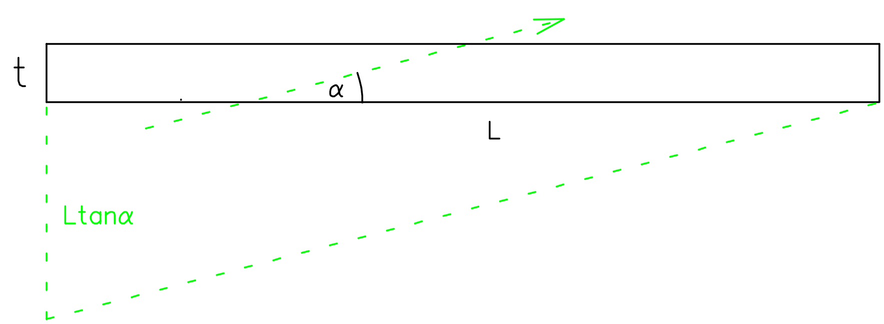

Figure 2.1: Counter geometry

The rate in the counter will then be:

$$R = \int f(x, y) \left(1 - e^{-\frac{t}{\lambda sin\alpha}}\right) dxdy \tag{2.2}$$

where y is taken over the interval $L\tan\alpha$. In the (bad) approximation that f(x,y) is a constant, this gives $R = fwL\tan\alpha(1 - e^{-\frac{t}{\lambda sin\alpha}})$. To get a feeling for what this implies, let's take the same assumptions for λ, L, and t as above. This yields the dependence for R/fw shown in Fig. 2.2.

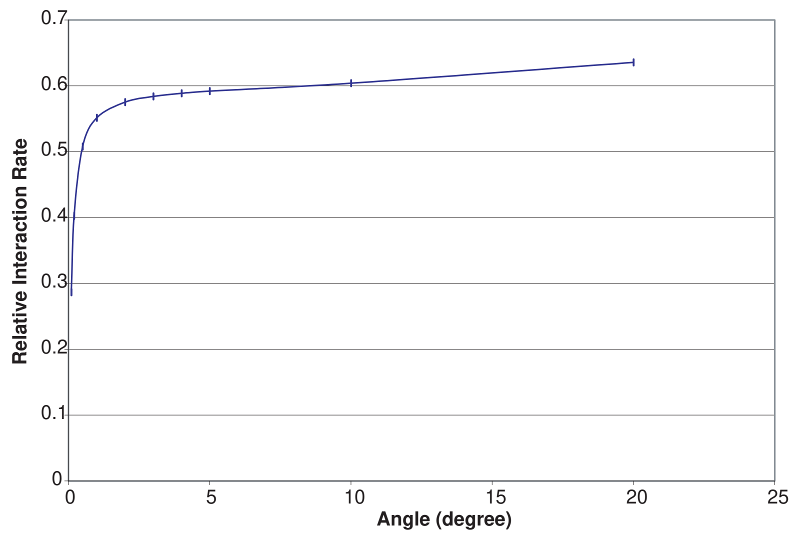

Figure 2.2: R/fw for very simplified assumptions

The values on this graph are to be compared with the 0.26 for the end-on case. So what we learn from this simplified case is (1) beyond about 2°, the average rate changes very slowly with further increase in angle and (2) the large angle rate is about 2.5 times the end-on case. There are a number of important caveats, the most important of which is that the assumption that $f(x, y)$ is not a function of y is not very plausible†.

3. Estimates of absolute rates for the 100mr × 5mr beam profile

3.1. A really crude estimate

To obtain an estimate of the absolute rates through the counters, one can turn to the Addendum to TN058[3]. I create Table 3.1 of overall fractional inclusions by adding the first few rows of Tables 1 and 2 in that paper, weighted by the fractions of incident neutrons each represents, and dividing by the similarly weighted average of the total surviving neutrons in the beam.

From Table 3.1 , one has 1.74×10^{-4} of the beam outside a rectangle of dimension 16cm by 180cm at 14m. Similarly one has a fraction 1.26×10^{-4} outside a rectangle 20cm by 180 cm. That means that one must have 0.48×10^{-4} of the beam within strips from 8 to 10cm above and below the beam and 180cm wide. Thus, in 1cm strips near ±9cm, there should be $\sim 1/2$ of this amount, or 2.4×10^{-5} of the beam. A similar exercise on the vertical strips near ±100cm, yields $\sim 3.90 \times 10^{-6}$ on the sides. Adding up the vertical

† Another assumption whose effect needs to be checked is that the neutrons have no angle in the x-z plane. Take an average angle given by 2×(beam half width halfway through the DS beampipe + beam half width halfway through the last collimator) divided by the ΔZ from the middle of the last collimator to this point), all divided by $\sqrt{12}$, i.e. $\overline{tan\beta} = 2(75 + 37.5)/(750\sqrt{12}) = .0866$, or $\overline{\beta} = 4.95°$ The path length in the scintillator should be $\approx t/(\lambda sin\alpha cos\beta)$. This turns out to be only a 0.4% effect, so can be ignored.

Table 3.1: Fraction of total neutrons in units of 10^{-6} outside the indicated areas (for Case 1). From Ref. 3 and data supplied by J. Doornbos.

	x(cm)	x(cm)	x(cm)	x(cm)	x(cm)	x(cm)	x(cm)
y(cm)	60	70	80	90	100	110	120
6	145398	50579	2227	466	417	397	385
7	145231	50393	2027	258	206	183	171
8	145164	50317	1946	174	121	97	84
9	145142	50291	1919	145	91	67	53
10	145128	50275	1901	126	72	47	33
11	145120	50266	1891	116	61	36	22

and horizontal strips gives 2.79×10^{-5} of the beam, or, taking 1.324×10^{10}n/sec for the beam flux (see Section 6), 0.37 MHz/cm of neutrons in the region of these counters. Now by the discussion in Section 2, the resulting rate in the counters will be ~ 0.6 of this or $\sim$ 222kHz. Note that this rate is almost linear in the thickness of the counters †.

This is pretty small compared to the rates from K_L decays. But before we decide to move the counters inward, we need a better characterization of $f(x, y)$. We address this below.

3.2. The next approximation

We need directional information on the halo neutrons to make progress. One could try the assumption that all halo neutrons come from scattering in the last collimator. This is a more realistic but more pessimistic assumption. The center along Z of this collimator is 750cm from the origin and the vertical extent of the collimator at this point is about +/-3.5cm. Thus if the far end of the DS beampipe CPV is at 1600cm, at +/-9cm, the nominal position of the counter, one is probing down to y=6.3cm (@ z=1400cm), at which point one has a total of $\sim$ 4 times the halo flux as is the case for the 9cm entries. One can get an approximate result as follows. The projections along Z for various y values are shown in Table 3.2, along with several other quantities needed for the rate calculation.

For each ΔZ interval, the average angle of incidence of neutrons scattering off the opposite face of the last collimator is given, along with the fraction of neutrons that count in the scintillator, assuming a 3mm thick counter and a 100cm absorption length. The local fractional density is obtained by subtracting successive entries in the X=100cm column of Table 3.1. This number is next multiplied by the beam rate of 1.324×10^{10}/sec (see Section 6) and finally this rate is multiplied by the fraction interacting. The total, 0.584 MHz is the rate in the horizontal planes of scintillator. This is about 3 times the rate given by our first, cruder, approximation for these counters. To get the total rate we must add the increment for the vertical counters at the sides. These rates are obtained in the same way

† For a thickness of 0.15cm the rate is 0.502 of that of the 0.3cm counter, for a 0.6cm counter, the rate is 1.983 of that of the 0.3cm counter.

Table 3.2: Rough calculation of neutron flux in the counters above and below the beam assuming all halo from last collimator. ΔZ is the distance along Z between the points that correspond to the Y_{equ} heights at 14m, assuming that all rays come from the opposite side of the last collimator. $f_{int} \equiv 1 - e^{-\frac{t}{\lambda sin\Theta_{av}}}$, $N_{beam} = 1.324 \times 10^{10}$/sec

Y_{equ}	ΔZ	Θ^y_{av}	f_{int}	$f(y)/N_{beam}$	$f(y)$	$R(MHz)$
9cm	0cm					
		0.92°	0.171	0.30×10^{-4}	0.397 MHz	0.067
8cm	65cm					
		0.84°	0.185	0.85×10^{-4}	1.13 MHz	0.208
7cm	143cm					
		0.77°	0.198	1.18×10^{-4}	1.56MHz	0.309
6.3cm	200cm					
Total						0.584

as those of the top and bottom counters, taking into account that the center of the last collimator is at $x \sim \pm 51$cm. Table 3.3 gives the calculation.

Table 3.3: Rough calculation of neutron flux in the counters at the sides of the beam assuming all halo from last collimator.

Y_{equ}	ΔZ	Θ^x_{av}	f_{int}	$f(x)/N_{beam}$	$f(x)$	$R(MHz)$
100cm	0cm					
		11.0°	0.017	0.54	0.715	0.012
90cm	53cm					
		10.3°	0.017	17.74	23.5	0.399
80cm	115cm					
		9.5°	0.018	640	640	11.53
70cm	186cm					
Total						18.2

This gives an enormous rate in the side counters, orders of magnitude greater than that of the first approximation! As will be seen below, this is too pessimistic. The error arises from the assumption that all scattering takes place at the center of the last collimator. It leads one to access part of Table 3.1 populated by neutrons coming directly from the production target. In fact **none** of these actually go beyond an 18cm $\times$ 200cm rectangle at 16m from the target, which is my assumed downstream limit of these CPV counters.

3.3. Estimate using Monte Carlo neutrons

To make a proper estimate one needs better information about the neutron directions and the correlations between the directions and positions. Jaap Doornbos kindly provided the output files used as a basis for Ref. 2. One can intersect the neutrons with the counter planes and find the actual path-length through the counter for each one. For Case 1, I have calculated the number of neutrons passing through the top/bottom and side counters and the thickness of scintillator through each passes. Fig. 3.1 gives the number and path-length distribution for the neutrons stemming from Jaap's run of incident neutrons with momentum greater than 750 MeV/c.

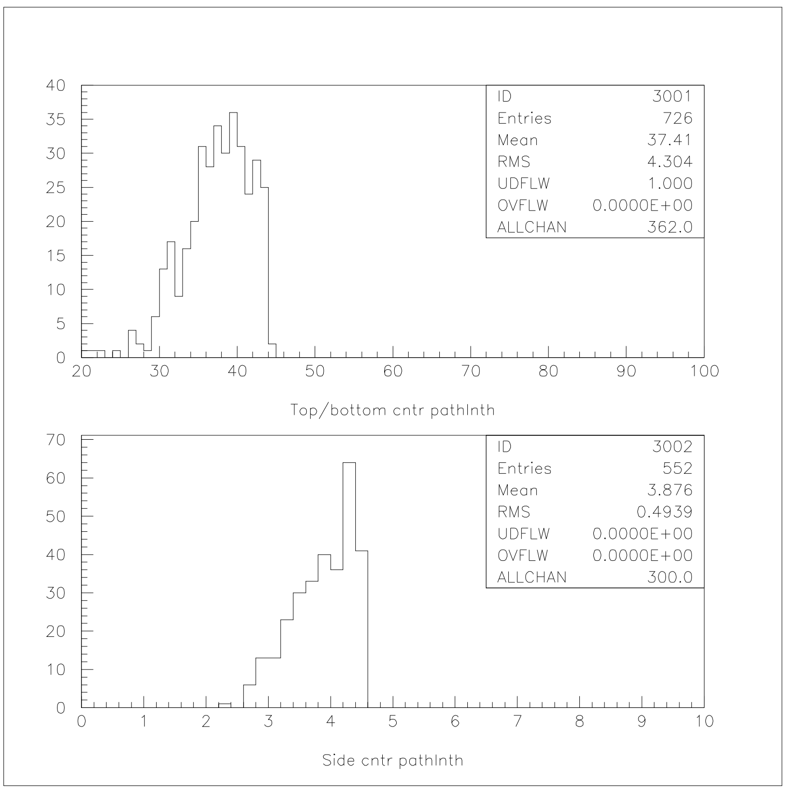

Figure 3.1: Halo trajectories through the DS beampipe CPV counters for the high energy run (upper plot is the path-length distribution for the top/bottom counters and lower plot is the corresponding distribution for the side counters).

One sees 362 neutrons pass through the top/bottom counters with average path-length of 37.41cm, whereas 300 neutrons pass through the side counters, with average path-length of 3.88cm. These are large numbers considering that the counters are only 3mm thick. On average then this sample gives 135.4 counts in the top/bottom counter and 11.6

counts in the side counters‡. The normalization is that these events correspond to 3.905M neutrons in the beam. In one spill, according to Section 6, one has 1.48×10^{10} high energy neutrons, and the spill is 2.7 nsec long. Therefore one must multiply these numbers by $1.44 \times 10^{10}/(3.905 \times 10^6 \cdot 2.7) = 1369$ to get 185.4kHz in the top/bottom and 15.9kHz in the side counters. Note that for this calculation neutrons coming directly from the target must be weighted[1] by a factor 80 and those whose last scatter is in the spoiler must be weighted by a factor 4.

Fig. 3.2 gives the corresponding information for the neutrons stemming from Jaap's run of incident neutrons with momentum less than 750 MeV/c.

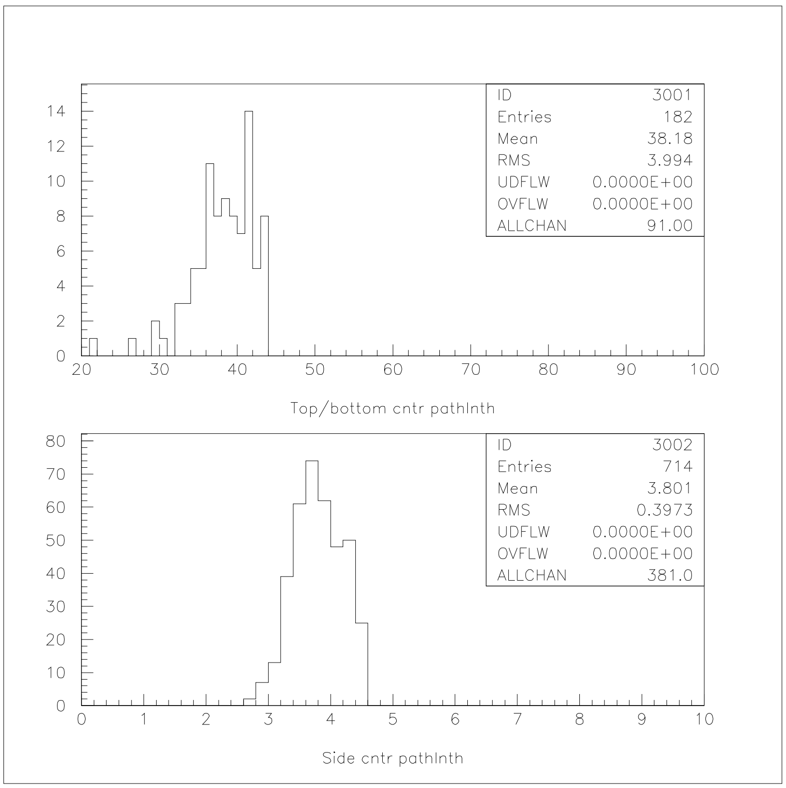

Figure 3.2: Halo trajectories through the DS beampipe CPV counters for the low energy run.

In this case 91 neutrons pass through the top/bottom counters with average path-length of 38.18cm, whereas 381 neutrons pass through the side counters, with average path-length of 3.80cm. On average then this sample gives 34.7 counts in the top/bottom counter and 14.5 counts in the side counters. The normalization is that these events correspond to 2.857M neutrons in the beam. In one spill, according to Section 6, one has

‡ Here I use a slightly more conservative estimate of the efficiency of the counters than above, i.e. 1%/cm.

2.13×10^{10} low energy neutrons, and the spill is 2.7 nsec long. Therefore one must multiply these numbers by $2.13 \times 10^{10}/(2.857 \times 10^6 \cdot 2.7) = 2763$ to get 95.9kHz in the top/bottom and 40.0kHz in the side counters.

The total rate in the top/bottom counters are therefore 281.2kHz and in the side counters the rate is 55.9kHz. Overall, the rate in the DS beampipe CPV is then 337.1kHz.

Now this rate doesn't seem too daunting compared with the 7.7MHz due to kaon decays. So one might ask the question – could we move the CPV counters closer to the beam and realize a higher acceptance. Table 3.4 shows the results for moving the top and bottom counters in from ±9cm by 1 cm intervals to ±6cm and also far moving them out by 1cm to ±10. Note that as one gets closer to the beam, the rates in the CPV go up for two reasons: more neutrons go through them and on the average they go through at more and more oblique angles.

Table 3.4: Rates in the DS beampipe CPV as a function of the vertical spacing of the counters. The rates are shown separately for incident neutrons with $p > 750\,\mathrm{MeV/c}$ (hi) and those with $p < 750\,\mathrm{MeV/c}$ (lo).

$\frac{1}{2}\Delta x/y$ (cm)	top+bottom rate hi/lo/tot (MHz)	side rate hi/lo/tot (MHz)	total rate hi/lo/tot (MHz)
100/10	0.108/0.042/0.150	0.016/0.040/0.056	0.124/0.083/0.207
100/9	0.185/0.096/0.281	0.016/0.040/0.056	0.201/0.136/0.337
100/8	0.418/0.240/0.658	0.015/0.040/0.055	0.433/0.280/0.713
100/7	.98/0.580/1.56	0.265/0.039/0.304	1.24/0.62/1.86
100/6	3.08/2.00/5.08	0.012/0.036/0.048	3.09/2.03/5.13

Fig. 3.3 shows the behavior of the total rate (top + bottom + 2 sides) as a function of the vertical position of the top/bottom counters. Note that one doesn't approach the K_L decay rates until moving in to the $\sim \pm 6$cm position.

Table 3.5 and Fig. 3.4 contain the corresponding information for moving the side counters in and out, this time by larger intervals.

Note that the nominal horizontal extent of the beampipe in our parameter list is 170cm which corresponds to the ±85cm point. At this width, the rates are more than 17 MHz, which is clearly unsustainable. There is a major upturn in rates when one gets within ±90cm. This is a little surprising because the extent of a ±50mr beam at 16cm (the downstream end of the calorimeter) is only ±80cm. The explanation lies in the finite horizontal extent of our production target. This can be seen in Fig. 3.5 which gives the distribution of horizontal positions at 16m for neutrons within ±9cm vertically at 16m vs the horizontal position at 0. The projected width of the target is about 7cm, can be seen in the distribution. The neutrons shown are those that come directly from the production target without any scattering. The vertical lines on the figure are drawn at ±90cm. One can see that there are events beyond ±90cm that come directly from the target. These outlying events can be seen to be correlated with neutrons that begin on the opposite side of the production target.

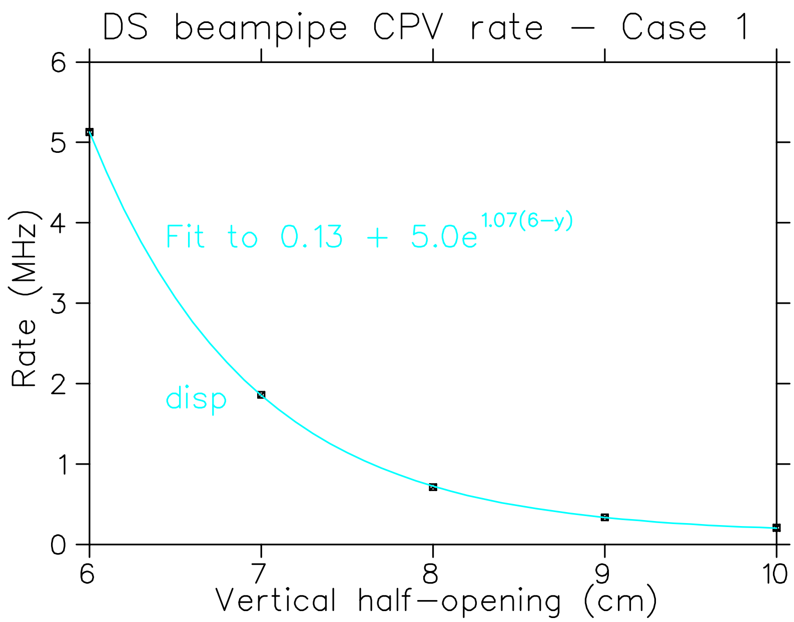

Figure 3.3: Rates in the DS beampipe CPV as a function of the vertical distance of the top and bottom counters from the center of the beam. The side counters are fixed at ±100cm. The solid line is a fit to an exponential plus a constant: $(5.00e^{1.066(6-y)} + 0.132)$MHz

Table 3.5: Rates in the DS beampipe CPV as a function of the horizontal spacing of the counters. The rates are shown separately for incident neutrons with $p > 750\,\mathrm{MeV/c}$ (hi) and those with $p < 750\,\mathrm{MeV/c}$ (lo).

$\frac{1}{2}\Delta x/y$ (cm)	top+bottom rate hi/lo/tot (MHz)	side rate hi/lo/tot (MHz)	total rate hi/lo/tot (MHz)
110/9	0.189/0.097/0.286	0.005/0.018/0.023	0.194/0.115/0.309
100/9	0.185/0.096/0.281	0.016/0.040/0.056	0.201/0.136/0.337
95/9	0.181/0.094/0.275	0.050/0.108/0.158	0.231/0.202/0.433
90/9	0.180/0.093/0.272	1.18/1.95/3.14	1.36/2.04/3.41
85/9	0.175/0.091/0.267	5.84/9.28/15.12	6.02/9.37/15.39
80/9	0.170/0.088/0.258	14.51/22.34/36.85	14.68/22.43/37.11

One can see the contribution of various sources to the outlying events in Fig. 3.6 and Fig. 3.7. These show the number of events hitting the side counters (unweighted) from each source for various horizontal positions of these counters. The upper left distributions are for the 100cm (canonical) setting. The upper right is for the the 95cm setting, the lower left for 90cm and the lower right for 85cm.

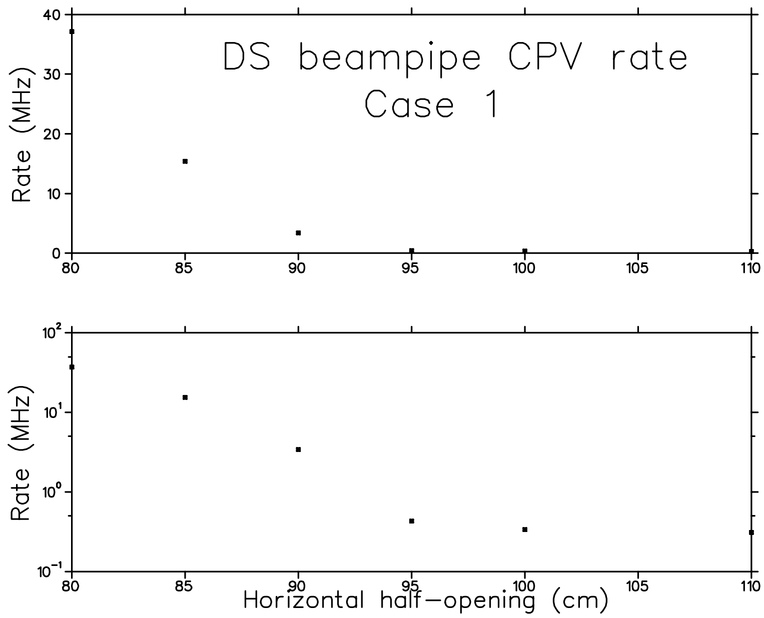

Figure 3.4: Rates in the DS beampipe CPV as a function of the horizontal distance of the side counters from the center of the beam. The top and bottom counters are fixed at ±9cm. Nominal position of eye-pipe is shown as a dotted vertical line. Results are shown in both linear and semi-log form.

3.4. Conclusions for the 100mr × 5mr beam

It's clear that from the point of view of rates in the CPV, one can't sustain a beampipe only 170cm wide as in our parameter list. Fig. 3.4 indicates that a width of much less than 190cm is not safe. On the other hand, from the point of view of CPV rates, one could probably stand a vertical separation of 16cm. I have calculated the rates for a "practical" case of 190cm × 16cm: These are 648kHz for the top/bottom counters and 157kHz for the sides, a total of 804kHz. As we will see later, for a 3mm thick counter, the neutron rates in the CPV may not turn out to be the limiting factor in determining the beam profile.

4. Rate estimates for alternative beam profiles

A number of suggestions for beam profiles that require a narrower downstream beampipe have been made.

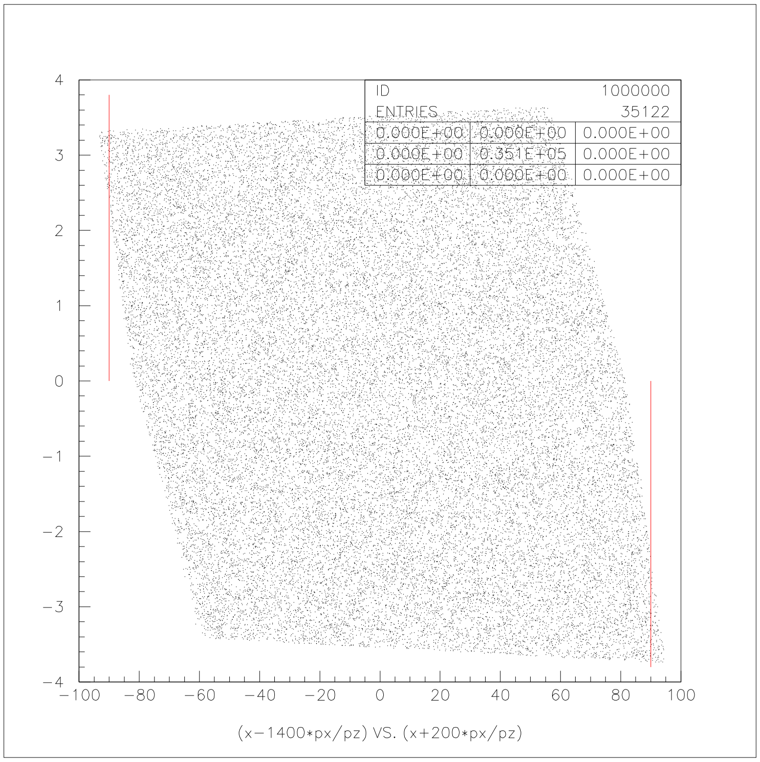

Figure 3.5: X-position of neutrons at Z=16m vs their x projected back to 0m. These neutrons are within ±9cm vertically at 16m. They are those that come directly from the production target without any further interaction. This is from low energy neutrons (incident energies from 10-262 MeV). The horizontal lines mark the ±90cm position.

4.1. Case 3, the 67mr × 7.5mr beam

I first prepare Table 4.1 that corresponds to Table 3.1. This table is not used in the present technical note, but it is of some general interest. It shows for example that David Jaffe correctly chose a point outside of which $\sim 10^{-4}$ of the beam lay at Z=14m. (He chose $|x|$ <78cm, $|y|$ <14cm).

Once again we use Jaap's trajectories to calculate the rates in the counters. For the (80,14) setting we get 234KHz in the T/B counters and 77KHz in side counters, for a total of 311KHz. This is pretty mild. Fig. 4.1 and Fig. 4.2 are the Case 3 plots corresponding to Case 1 plots Fig. 3.3 and Fig. 3.4.

For Case 3, also, it appears that the counters could be move toward the beam without being flooded by rates. I've calculated the rates in the "practical" case of (70,11). These come out to be 868KHz in the T/B counters and 300KHz in the side counters for a total of 1.17MHz.

But once again, this may not prove to be the dominating consideration in determining the size of the beampipe.

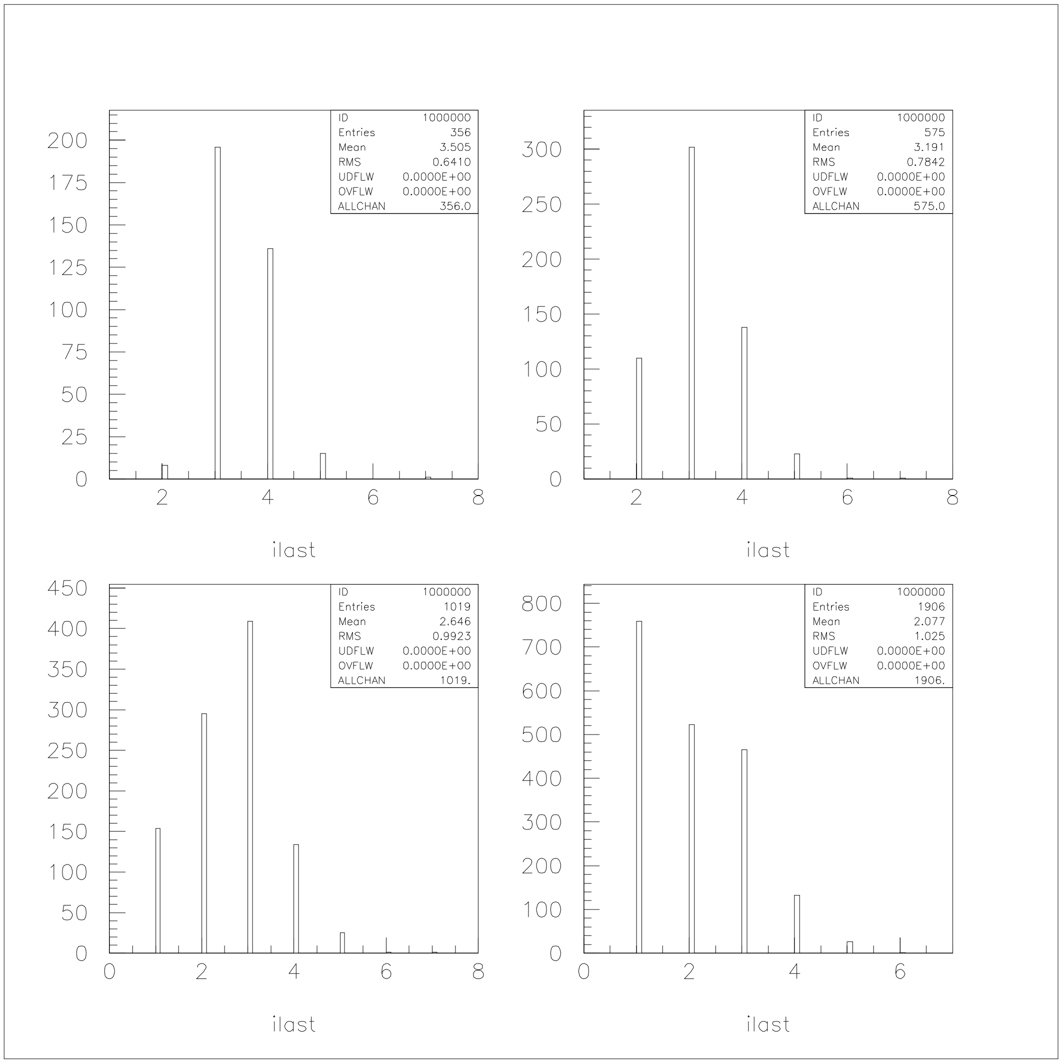

Figure 3.6: Contribution of various sources to the neutrons impinging on the side counters. The first bin contains events coming directly from the production target with no further scatters. These should be multiplied by a factor 80. The second bin are neutrons whose last scatter was in the spoiler. These should be multiplied by a factor 4. The next 5 bins are those that underwent a last scattering in the successive collimators. The upper left, upper right, lower left, and lower right correspond to the position of the side counters at $\pm$100cm, $\pm$95cm, $\pm$90cm, and $\pm$85cm respectively. This figure is for incident neutrons with energies between 10 and 262 MeV.

5. Other considerations

Scattered neutrons will inevitably give rates in other parts of the detector, and these can cause random vetoes. We also need to take account of these to get a complete context for assessing the effect of varying the beam profile and the DS beampipe CPV configuration.

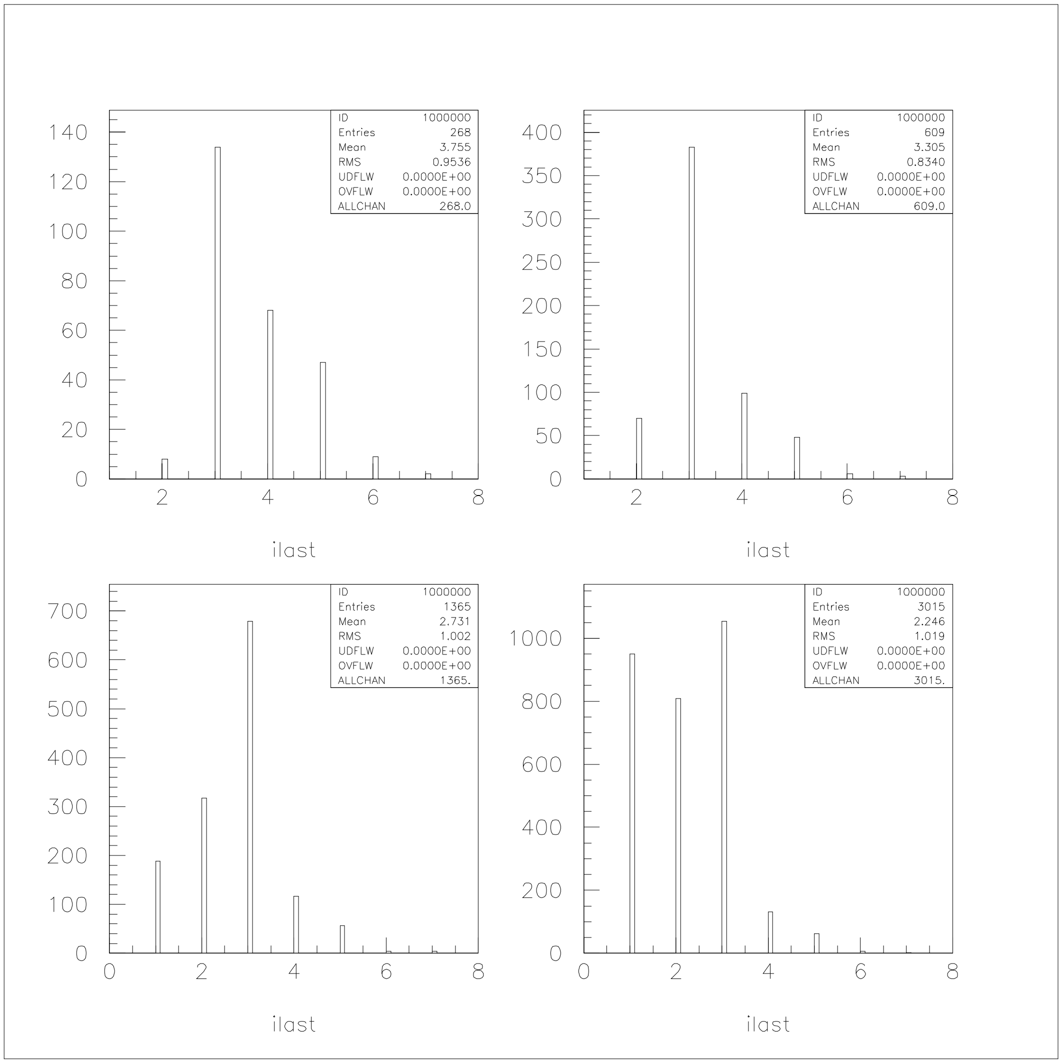

Figure 3.7: Same as Fig. 3.6, except these are for neutrons with incident energy greater than 262 MeV (750 MeV/c).

Note that it is advantageous to intercept halo neutrons in the catcher because it is much less sensitive to them than is any of the other systems.

5.1. Case 1

First let's determine how many neutrons are outside a kind of minimal catcher profile. The KOPIO parameter file has the catcher face 13m downstream of the preradiator face. Let's take the height (20cm) and the width (400cm) from the draft TDR. Then for Case 1, using Jaap's files, the high energy rate turns out to be 10.48MHz and the low energy rate 6.99MHz, for a total of 17.4MHz. For a 10nsec veto gate, this would yield a 17.4% loss of sensitivity. For Case 3, the situation would be disastrous unless the catcher were made higher – the total rate would be 706 MHz! If one changes the dimensions of the catcher in proportion to the beam profile, i.e. makes it 267cm wide by 30cm high, the rate would be

Table 4.1: Fraction of total neutrons in units of 10^{-6} outside the indicated $|x|$ and $|y|$ limits (for Case 3). From Ref. 3 and data supplied by J. Doornbos.

	x(cm)	x(cm)	x(cm)	x(cm)	x(cm)	x(cm)
y(cm)	70	80	90	100	110	120
10	407	323	288	279	277	277
11	309	222	185	176	173	173
12	246	156	118	108	106	105
13	212	122	83	73	70	70
14	188	97	58	47	45	44
15	177	85	45	34	31	31
16	172	80	39	29	26	25
17	169	77	36	25	22	22

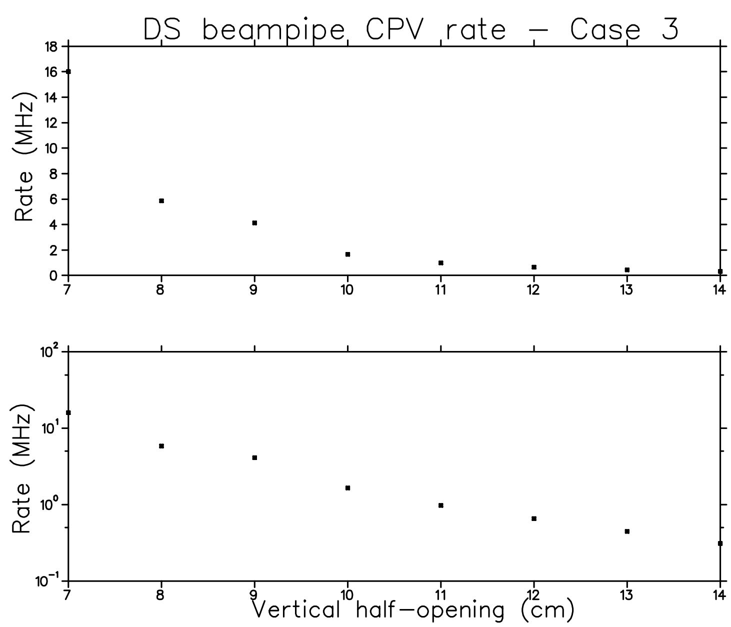

Figure 4.1: Rates in the DS beampipe CPV as a function of the vertical distance of the top and bottom counters from the center of the beam. The side counters are fixed at ±80cm. Results are shown in both linear and semi-log form.

24.4MHz. Thus one would need to make the catcher somewhat bigger than proportional, to recover the rate of Case 1 (*e.g.* 300cm × 35cm would be more than sufficient).

Returning to Case 1, we can get an idea of how the 17.4MHz could be reduced by looking at Fig. 5.1 which shows the high energy neutrons outside the catcher. For reasons

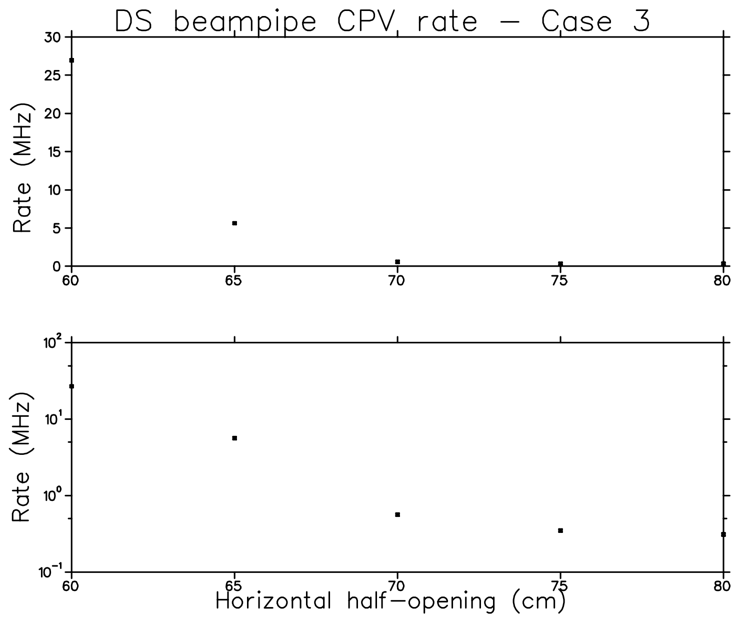

Figure 4.2: Rates in the DS beampipe CPV as a function of the horizontal distance of the side counters from the center of the beam. The top and bottom counters are fixed at ±14cm. Results are shown in both linear and semi-log form.

discussed below, there's a cut limiting these neutrons to be within the profile of the DS beampipe CPV at 16m. One can see immediately that there's no point in making the catcher any wider, but it's clear that one would gain quickly as the height of the catcher increased. To properly assess the gains one must eliminate far flung neutrons that will certainly interact in the detector before striking an extended catcher. Thus the cut mentioned above to eliminate neutrons that strike the DS beampipe CPV removes neutrons that no catcher is likely to see. The latter neutrons, which will presumably convert in the preradiator, calorimeter or DS vetoes constitute 2.67MHz of the total 17.4MHz outside of the TDR catcher profile. The residual, 14.8MHz is the portion that can be greatly reduced by increasing the vertical size of the catcher. Table 5.1 shows the two components of rate as a function of the catcher height (for Case 1).

Clearly there is $\sim$ 2MHz of rate that is rather insensitive to adjusting the catcher height. But increasing the catcher height from 20cm to 32cm reduces the "inside" rate from 14.76MHz to 440KHz and the total 17.43MHz discussed above to 2.45MHz. Increasing the catcher dimension seems a clear win, but one must check the effect on background induced by the larger photon veto inefficiency this will cause for a small amount of phase space.

The conclusion so far is that for Case 1, David's choice of CPV dimensions gives quite acceptable neutron random rates in all parts of the detector as long as the catcher is made higher. However we had noted that as far as the rates in the DS beampipe CPV were concerned, we could use a smaller opening, 190cm $\times$ 16cm instead of 200cm $\times$ 18cm. So let's go through the same exercise on rates in the detector for the smaller opening. Of course for the same size catcher (400cm $\times$ 20cm) the total rates outside the catcher are the same. Moving the CPV (and the beampipe and detectors) inward just changes the fraction of

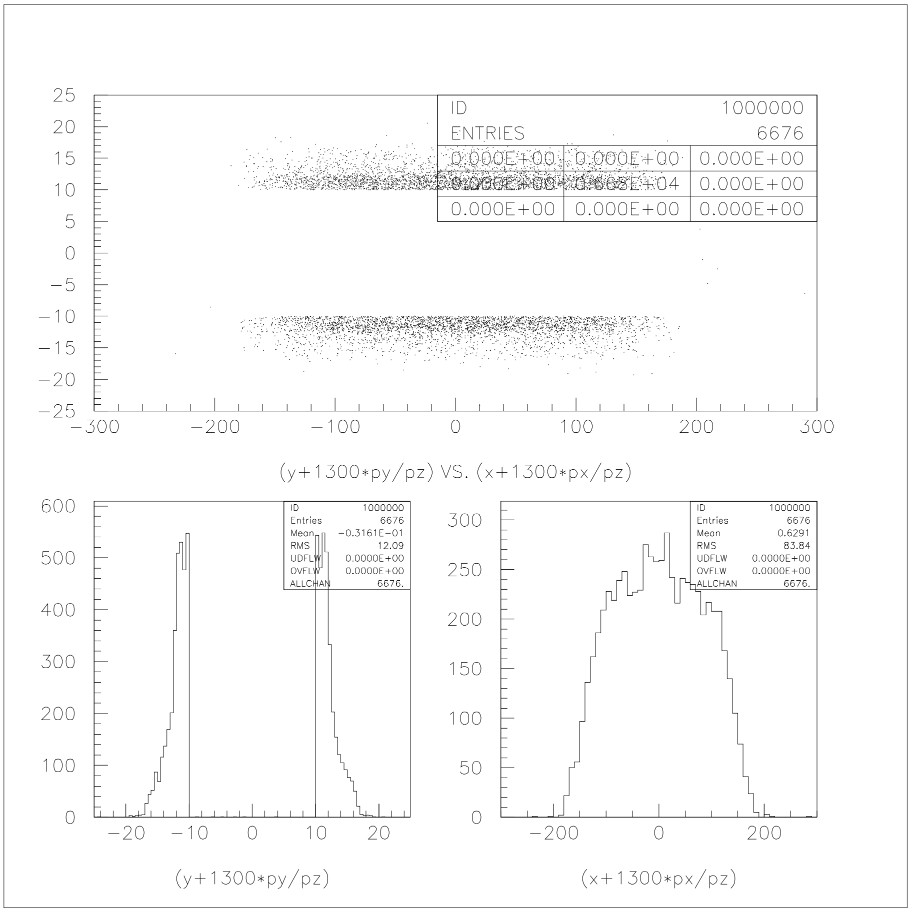

Figure 5.1: Distribution of events outside the TDR catcher for high energy neutrons within the DS beampipe CPV profile (200cm × 18cm at Z=16m). The 2-d plot and y and x projections are shown (for Case 1).

the neutrons that actually get back to the catcher. Now, instead of the split inside/outside = 14.76/2.67MHz, we find 13.39/4.03MHz. Enlarging the catcher quickly reduces the 13.39MHz, but the 4MHz of detector/DS veto rate changes more slowly. For example, if we make the catcher 32cm high as in the last example, the rates are 0.19/2.87MHz. So the rates in the detector and DS veto have gone up by 7% wrt the 200cm × 18cm case. This rise probably not a determining factor in the Case 1 configuration, but we need to keep our eye on this as we vary the beam profile.

One should keep in mind that it's preferable to intercept neutrons in downstream vetoes, rather than by the active detector elements. For one thing the effect on the trigger of such randoms is more straightforward. For another, any neutron detected beyond the sweeping magnet is a candidate only for a background photon, so that the anticoincidence timing gate can be made very narrow. For neutrons detected in the CPV, one must use a wider, charged-particle gate so that the random veto loss is more severe.

Table 5.1: Rates outside the catcher profile for various catcher heights (for Case 1). The first row is the TDR case. "Inside" means the neutrons are limited to those passing inside an 18cm × 200cm rectangle at Z=16m. "Outside" means those outside that rectangle at 16m.

Catcher height	Total (MHz)	Inside CPV (MHz)	Outside CPV (MHz)
20cm	17.43	14.76	2.67
24cm	7.96	5.44	2.52
28cm	4.31	1.83	2.47
32cm	2.89	0.44	2.45
36cm	2.20	0.05	2.14
40cm	1.99	0.03	1.96

5.2. Case 3

Let's take the "practical" version of Case 3, in which the DS beampipe CPV dimensions are ($\pm$70cm, $\pm$11cm). Fig. 5.2 contains the plots corresponding to Fig. 5.1 for this case.

It's clear that with this DS beampipe CPV dimension there's no need to make the catcher wider than 300cm. Perhaps it can be as narrow as ~270cm. The rates in the case of a 270cm × 30cm catcher are 24.1MHz outside the catcher, of which 15.0MHz is within the DS beampipe CPV (i.e. will show up the the DS vetoes) and 9.1MHz is outside (i.e. will show up in the detector).

Table 5.2: Rates outside the catcher profile for various catcher sizes (for Case 3). 'Inside" means the neutrons are limited to those passing inside a 22cm × 140cm rectangle at Z=16m. "Outside" means those outside that rectangle at 16m.

Catcher height	Catcher width	Total (MHz)	Inside CPV (MHz)	Outside CPV (MHz)
30cm	270	24.08	15.01	9.08
30cm	300	22.91	14.97	7.94
35cm	270	13.13	4.26	8.87
35cm	300	11.76	4.21	7.55
40cm	270	9.23	0.49	8.74
40cm	300	7.72	0.41	7.31

Table 5.2 shows the rates for variations of the catcher dimensions. Note that as in Case 1, it is possible to reduce the rates that end up in the downstream vetoes by enlarging

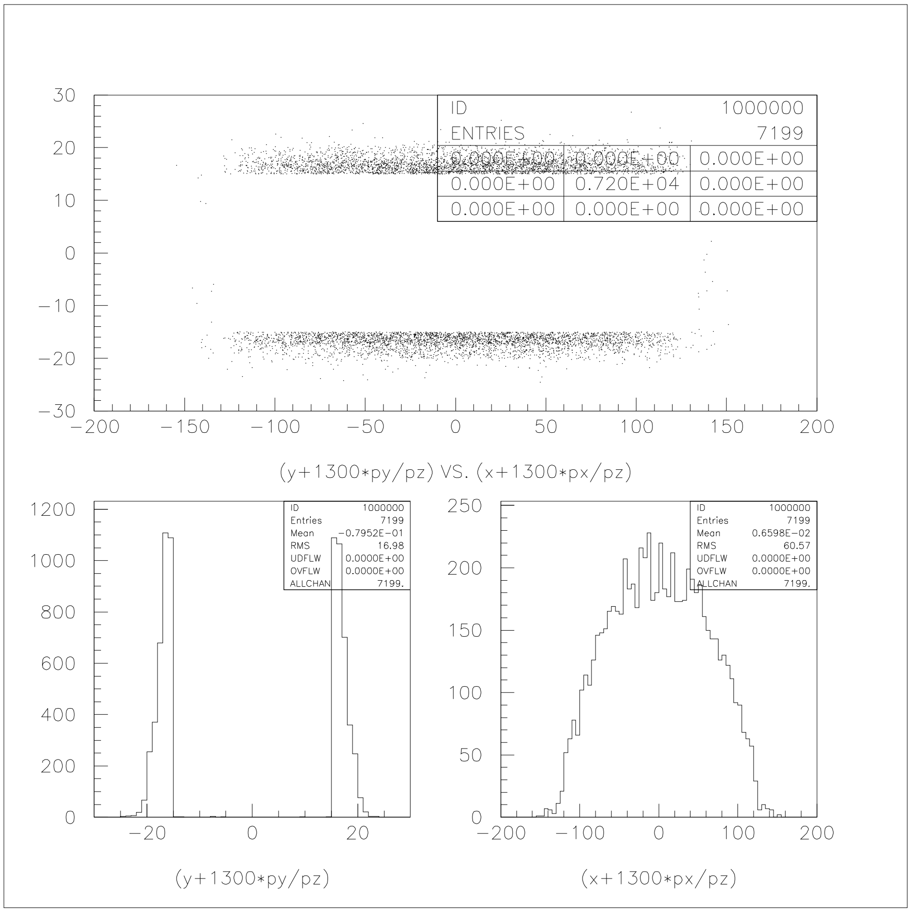

Figure 5.2: Distribution of events outside a catcher scaled for Case 3 ($\pm$ 133.3cm, $\pm$ 15cm) for high energy neutrons within the DS beampipe CPV profile ($\pm$ 70,$\pm$ 11cm). The 2-d plot and y and x projections are shown.

the catcher, and that the rates in the preradiator, calorimeter, etc. respond more slowly. However there's a significant difference in the latter absolute rates. These are in the neighborhood of 8MHz instead of the ~2MHz we found for Case 1. What this is telling us is that the CPV dimensions are probably too small. I.e. in Case 3, it is definitely the detector rates, rather than the DS beampipe CPV rates that will determine the dimensions of the latter. If we go all the way back from the "practical" version of Case 3 to approximately David Jaffe's dimensions (I use 28cm $\times$ 160cm), the rates are 7.7MHz in total, of which about half are within the profile of the DS beampipe CPV and half outside it.

Where do these rates occur in the detector? Fig. 5.3 shows the distribution on the Z=16m plane of neutrons outside the perimeter of the DS beampipe CPV for the two options discussed so far. One can see, particularly in the latter case for the low energy neutron sample, most of the rates are in in the horizontal swath adjacent to the beam. One would need to widen the beampipe to $\sim$188cm to reduce the outside rates by a factor 2. For the high energy neutrons, the rates are more equally divided between the vertical

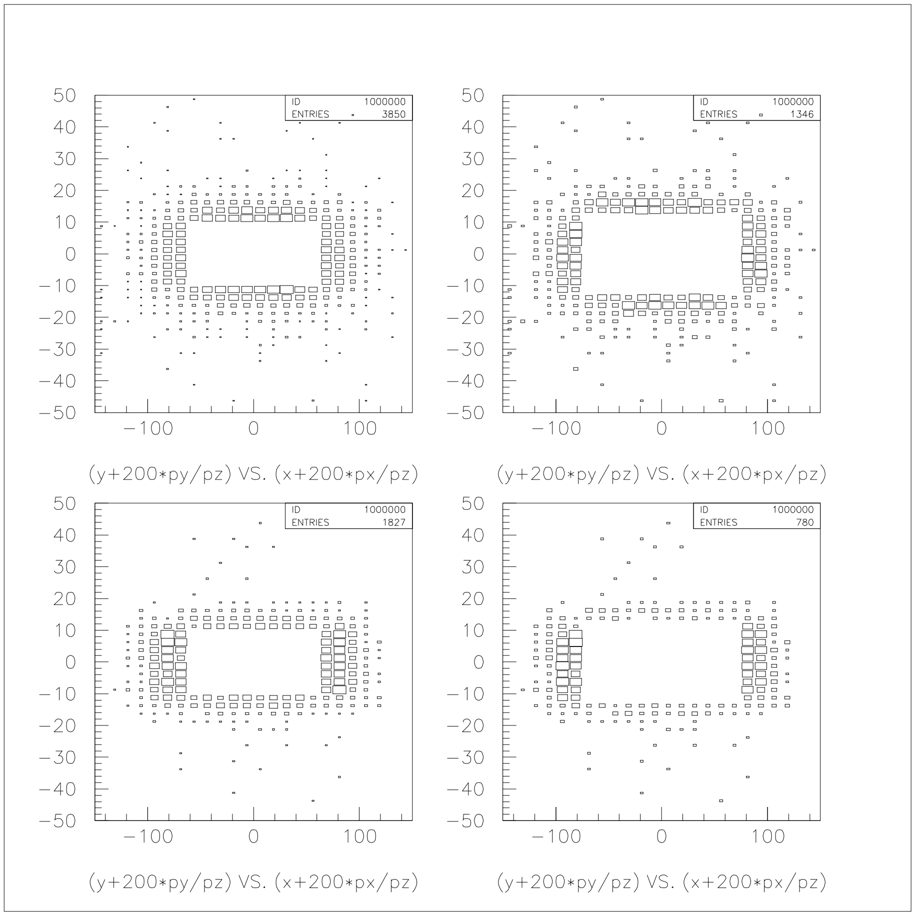

Figure 5.3: Distribution of neutrons outside the DS beampipe CPV at the plane Z=16m (i.e. the DS end of this CPV). The top plots are for the high energy neutrons and the bottom plots for the low energy ones. The left plots show the case of a 22cm $\times$ 140cm CPV and the right plots that of a 28cm $\times$ 160cm CPV.

and horizontal. To reduce them by a factor 2 would require not only widening the CPV to 188cm, but making it higher by about 3cm.

6. Appendix 1 - Notes on absolute flux normalization

Note there's a typo in Ref. 2 for the total neutron/proton yield. Table 4 on page 142 of the KOPIO proposal[4] gives a neutron flux of 1.66×10^{-6}/proton/μsr for energies above 10 MeV. However the partial yields of 1.11×10^{-6}/proton/μsr for neutron energies from 10-262 MeV and 0.55×10^{-6}/proton/μsr for neutron energies above 262 MeV given in Ref. 2 are correct. Jaap translates these yields into fluxes by multiplying by the solid angle (500 μsr) and by the proton flux (10^{14}/pulse). He also takes into account the absorption of the lead spoiler. I believe he does this in the following way. He generates 50M events isotropically† into a solid angle of 3360μsr. Of these presumably a fraction 500/3360 go into the 500μsr of the beam acceptance. Thus a total of 7.44M neutrons are generated into the beam opening angle. Since 3.905M high energy neutrons survive, the spoiler survival probability for these is 52.5% and since 2.857M low energy neutrons survive, the spoiler survival probability for these is 38.4%. These numbers are consistent with the statements in Ref. 2, and I repeat them here because they are smaller than the numbers we've used in the past and result in lower total rates.

The high energy neutron flux for one AGS pulse is $\frac{0.55\cdot 10^{-6}\times 500\times 10^{14}\times 3.905\cdot 10^{6}}{7.44\cdot 10^{6}} = 1.4433\times 10^{10}$. The corresponding low energy flux is $\frac{1.11\cdot 10^{-6}\times 500\times 10^{14}\times 2.857\cdot 10^{6}}{7.44\cdot 10^{6}} = 2.1312\times 10^{10}$. These are a little lower than those given in Ref. 2, due to the use of exact numbers of surviving neutrons instead of 4M and 3M for the high and low energy neutrons respectively.

There should be some corrections to this. There's one due to the fact that the incident high energy neutrons contribute a little to the low energy yield. This turns out to be a 0.2% effect so can be ignored. Another has to do with the fact that it's possible that neutrons heading outside the beam solid angle could conceivably scatter back into it. I don't know how large such an effect might be.

Adding the high and low energy absolute fluxes given above yields 3.575×10^{10} neutrons/pulse. If we then assume a 2.7 second spill, we have 13.24 GHz of beam neutrons.

Note that the normalizations are slightly dependent on the beam profile. For Case 1, there are 3,904,939 surviving high energy neutrons and 2,856,907 surviving low energy neutrons. For Case 3, the corresponding numbers are 4,146,898 and 2,897,701 respectively. These imply that the high and low energy neutron fluxes for one AGS pulse are 1.5328×10^{10} and 2.1616×10^{10} respectively. The spoiler survival probabilities are 55.7% and 38.9% respectively.

7. Appendix 2 - Neutron Rates in the BV, etc.

Let's consider the rates due to neutrons headed outside the preradiator. My assumption is that all of these will count either in the the BV or the veto counters surrounding the preradiator. Presumably this is a conservative assumption. It turns out that in both Case 1 and Case 3, there are no events outside the perimeter of the preradiator ($\pm$2m) at Z=14m. This translates into a 90% CL limit of 9.5KHz. This is not quite the whole story, however, because *some* of the beam halo strikes the upstream wall of the BV. If we define this as all neutrons outside an 18cm $\times$ 200cm rectangle at Z=10m, in Case 1 we find a rate of 52.2KHz.

† No doubt a more accurate assumption should be tried.

8. Appendix 3 - Possible improvements to the estimates in this technical note

1. Jaap Doornbos's simulations could be redone taking account of the variation in neutron flux and spectrum as a function of production angle.
2. The results of a real simulation of neutron interactions with scintillator could be substituted for the 1%/cm rule.

1. J. Doornbos, KOPIO TN049.
2. J. Doornbos, KOPIO TN058.
3. J. Doornbos, KOPIO AD058.
4. I-H. Chiang, et al., "KOPIO - a search for $K^0 \to \pi^0 \nu\bar{\nu}$", Oct. 1999.